Eur. Phys. J. B **41**, 11–21 (2004)
DOI: 10.1140/epjb/e2004-00288-4

THE EUROPEAN PHYSICAL JOURNAL B

Real space renormalization group with effective interactions: applications to 2-D spin lattices

M. Al Hajj[a], N. Guihéry, J.-P. Malrieu, and B. Bocquillon

Laboratoire de Physique Quantique, IRSAMC/UMR5626, Université Paul Sabatier, 118 route de Narbonne, 31062 Toulouse Cedex 4, France

Received 1st March 2004 / Received in final form 11 June 2004
Published online 30 September 2004 –

Abstract. The Bloch's theory of effective Hamiltonians has been used to improve the Real Space Renormalization Group approach. The effective interactions between elementary blocks of a periodic lattice can be extracted from the knowledge of the spectrum of the dimers or trimers of blocks. The potentialities of the method are illustrated on a series of quasi 1-D and 2-D problems. The spin gap of two-leg ladders is calculated and an estimate of the impact of ferromagnetic couplings between two-leg ladders on the gap is presented. The method satisfactorily identifies the phase transitions in the 1/5-depleted square lattice as well as in the spin-frustrated Shastry-Sutherland lattice. The J_2/J_1 checkerboard lattice is studied and a location of the phase transition between the Néel phase and the dimer phase is proposed.

PACS. 71.10.-W Theories and models of many-electron systems – 71.15.Nc Total energy and cohesive energy calculations – 75.10.-b General theory and models of magnetic ordering

1 Introduction

The real-space renormalization-group has been suggested by Wilson as a seducing idea for the treatment of the electron or spin periodic lattices [1]. The proposal goes through the definition of blocks or supersites, which may in principle be identical or different but which define another lattice of a different scale. The basic idea was to reduce the Hilbert space by considering only a few eigenstates of the Hamiltonian in each block and the products of these selected eigenstates in the treatment of superblocks. If each block i bears a mean number m of particles on its n sites, one may solve the eigenvalue problem for each block with m particles on these n sites, defining a finite subspace of projector $P_{n,i}$

$$P_{n,i}HP_{n,i}\Phi_{k,i} = \mathcal{E}_k\Phi_{k,i}, \tag{1}$$

and one may retain only m states $\Phi_{k,i}$, for instance those of lowest energies. They define a m-dimensional space s_i on each block. For the treatment of the superblock, made of N blocks, one will consider the space $\mathbf{S_N}$ spanned by the products of the selected states $\Phi_{k,i}$ in each block, i.e.,

$$\mathbf{S_N} = s_1 \otimes \cdots \otimes s_i \otimes \cdots \otimes s_N. \tag{2}$$

Let call $P_{\mathbf{S_N}}$ the projector on this space. It is hoped that the diagonalization the corresponding truncated Hamiltonian $P_{\mathbf{S_N}}HP_{\mathbf{S_N}}$ will provide reasonable approximations of the exact eigenvalues for the N blocks. This idea is very elegant since it may be iterated by considering blocks of blocks, and so on. In general the problems at the different steps, i.e., for the different scales, are isomorphic and one converges to one of the accumulation points of the problem.

Unhappily the numerical efficiency of the algorithm is poor. It fails for instance on the elementary problem of the lowest eigenenergy of the one electron tight-binding Hamiltonian for the 1-D chain. The failure has led to abandon the original RSRG, and to the conception of a deeply different procedure, namely the Density-Matrix Renormalization-Group [2,3]. This last procedure is very efficient, but essentially limited to 1-D lattices. In a previous paper [4], two of the authors suggested a possible improvement of the RSRG technique by introducing effective interactions between the blocks, which they called RSRG-EI. They made use of the Bloch's theory of effective Hamiltonians [5] to define these effective interactions from the exact spectrum of the dimers or trimers of blocks. The few numerical simple illustrations given in reference [4] appeared to be very encouraging. The applications concerned spin lattices. The blocks involved odd number of sites and had a doublet ground state. This state was the only one retained, and therefore each block could be seen as an effective spin $S_z = \pm 1/2$. The method was applied to blocks of different sizes and the results were extrapolated with respect to the number of sites of the blocks.

The present paper illustrates the potentialities of the method for the study of quasi 1-D and of 2-D systems. The

[a] e-mail: alhajj@irsamc.ups-tlse.fr

study of the spin gap in a ferro-antiferromagnetic chain and in two-leg ladders allows one to discuss briefly some methodological points regarding a few degrees of freedom of the method concerning the shape of the blocks and the extraction of effective interactions from dimers or trimers of blocks. The applications to 2-D systems concern

- the impact of the weak interladder ferromagnetic interaction in $SrCu_2O_3$ on the spin gap of that lattice;
- the phase transition of the spin non-frustrated 1/5-depleted lattice;
- the phase transition occurring in the Shastry-Sutherland and checkerboard frustrated lattices.

It will be shown that the method provides a direct and elegant identification of the critical interactions, i.e., of the phase transitions for these three 2-D lattices.

2 The Bloch's theory of effective Hamiltonian and its use for the definition of effective interactions between blocks

2.1 Bloch's theory of effective Hamiltonians

The concept of effective Hamiltonians receives various definitions. Its most rigorous acception will be recalled here. In general the effective Hamiltonians are built by applying Quasi Degenerate Perturbation Theory to a given model space, after a proper partition of the Hamiltonian into a zero order H_0 operator and a perturbation operator $V = H - H_0$. The effective Hamiltonian is obtained at convergence of the perturbation expansion. Bloch has provided a more general formulation of this concept [5]. The Bloch's theory of effective Hamiltonians [5] is based on a one-to-one correspondence between two isodimensional subspaces. One considers first a m-dimensional model space, onto which one would like to build an effective Hamiltonian. This model space is spanned by selected configurations $|I\rangle$, which are supposed to play a privileged role in the wave functions $|\Psi_k\rangle$ of the exact Hamiltonian which are of special interest, for instance the lowest eigenstates. Let call S_0 the model space and P_0 its projector

$$P_0 = \sum_{I \in S_0} |I\rangle\langle I| \qquad I = 1, m. \tag{3}$$

The effective Hamiltonian will be built in the model space

$$H^{eff} = P_0 H^{eff} P_0 + 0(1 - P_0) H^{eff} (1 - P_0). \tag{4}$$

The maximum task that H^{eff} may fulfill is that its m eigenvalues are exact eigenvalues and that its eigenvectors are the projections of the corresponding exact eigenvectors in S_0. This means that if

$$H\Psi_k = \mathcal{E}_k \Psi_k, \qquad \forall\ k, \tag{5}$$

then

$$H^{eff} |P_0\Psi_k\rangle = \mathcal{E}_k |P_0\Psi_k\rangle, \quad k = 1, m. \tag{6}$$

The m eigenstates Ψ_k which are targeted by the effective Hamiltonian span the so-called target space [6] S of projector P, isodimensional to the model space, and the wave operator Ω sends from S_0 to S,

$$P = \Omega P_0, \qquad H^{eff} = P_0 H \Omega P_0. \tag{7}$$

The effective Hamiltonian is based on a correspondence between the model space and an isodimensional stable subspace of H.

Although the choice of S may be in principle arbitrary provided that Ω exists, i.e., that the projection of the eigenvectors $|\Psi_k\rangle$ of S have linearly independent projections on S_0, a rational choice of S satisfies the condition

$$\sum_{k \in S} ||P_0\Psi_k|| \qquad \text{maximum}, \tag{8}$$

i.e., the target space is spanned by the m eigenstates of H having the largest projections in the model space. Notice that these projections are not necessarily orthogonal, although $\langle\Psi_k|\Psi_l\rangle = \delta_{kl}$

$$\langle P_0\Psi_k|P_0\Psi_l\rangle \neq \lambda_k \delta_{kl}. \tag{9}$$

Let call the S the overlap matrix of these projections. The spectral definition of H^{eff} in the Bloch's formalism is

$$H^{eff} = \sum_k |P_0\Psi_k\rangle \mathcal{E}_k \langle P_0\Psi_k^{\perp}|, \tag{10}$$

where $\langle P_0\Psi_k^{\perp}|$ is the bi-orthogonal vector associated to $|P_0\Psi_k\rangle$. This effective Hamiltonian is not hermitian

$$\langle I|H^{eff}|J\rangle \neq \langle J|H^{eff}|I\rangle. \tag{11}$$

Hermiticity is a desirable property of transferable effective Hamiltonian. It can be restored by any kind of orthogonalization of the $|P_0\Psi_k\rangle$'s, either symmetrical using the least motion $S^{-1/2}$ transformation, as proposed by des Cloizeaux [7], or hierarchized according to the Schmidt procedure.

2.2 Definition of effective interactions in the RSRG method

The preceding formalism may be used to improve the original RSRG method. Again one defines blocks (which may be identical or different) of a moderate size n, such that their exact spectrum can be calculated. One selects for each block I a set of M low energy eigenvectors $\Phi_{k,I}$ $(k = 1, M)$. Then one will consider a dimer of blocks AB (or a trimer of blocks ABC), and a model space defined by the M^2 (or M^3) products

$$\Phi_{kl,AB} = \Phi_{k,A}\Phi_{l,B} \quad \text{or} \quad \Phi_{klm,ABC} = \Phi_{k,A}\Phi_{l,B}\Phi_{m,C}, \tag{12}$$

$$P_{S_{AB}} = \sum_{k=1,M} \sum_{l=1,M} |\Phi_{kl,AB}\rangle\langle\Phi_{kl,AB}|. \tag{13}$$

The basic idea consists in establishing the effective Hamiltonian in this model space in order to evaluate effective interactions between the vectors $\Phi_{kj,AB}$ and $\Phi_{gh,AB}$. One may eventually use the quasi-degenerate perturbation theory to second order

$$\langle\Phi_{kl,AB}|H^{eff}|\Phi_{gh,AB}\rangle = \langle\Phi_{kl,AB}|H|\Phi_{gh,AB}\rangle + \sum_{\substack{r \\ r\ and/or\ s>M}}\sum_{s} \frac{\langle\Phi_{kl,AB}|H|\Phi_{rs,AB}\rangle\langle\Phi_{rs,AB}|H|\Phi_{gh,AB}\rangle}{E^0_{gh,AB} - E^0_{rs,AB}}. \quad (14)$$

One sees from that formula that the effective Hamiltonians incorporates the indirect effect of the eigenstates of the blocks which have not been selected in the fragments. Rather than using this perturbative approach [8], we prefer to use blocks of a sufficiently small size, in order to solve exactly the dimer (or the trimer) Hamiltonian. Knowing its relevant eigenvectors $\Psi_{l,AB}$ (i.e., target space)

$$H_{AB}\Psi_{l,AB} = E_{l,AB}\Psi_{l,AB}, \quad (15)$$

one may use the spectral definition of the exact effective Hamiltonians (Eq. (10)) in order to calculate the effective interactions between the blocks A and B, i.e., the $\langle\Phi_{kl,AB}|H^{eff}|\Phi_{gh,AB}\rangle$ matrix elements. In the treatment of superblocks, consisting of n blocks, or of dimers of superblocks, consisting of $2n$ blocks, one uses the $\langle\Phi_{kl,IJ}|H^{eff}|\Phi_{gh,IJ}\rangle$ matrix elements between the blocks I and J. The same strategy is repeated till convergence, i.e., till the disappearance of some interactions and the invariance of other ones. At each step effective interactions are calculated from the dimer or trimer spectrum through the use of effective Hamiltonian theory.

2.3 Dimers versus trimers, the size complexity dilemma

For spin 1/2 systems in which each site bears one spin, up or down, obeying a Heisenberg Hamiltonian

$$H = \sum_{\langle i,j\rangle} 2J_{ij}(S_iS_j - 1/4), \quad (16)$$

the simplest application of the effective Hamiltonian theory will consist in

- the consideration of blocks composed of an odd $(2n+1)$ number of sites, such that their ground state is a non-degenerate doublet state;
- the reduction of the possible states of each blocks to this $S_z = \pm 1/2$ ground state. In such a case the unique degree of freedom in the block is its spin, the block can be seen as a supersite of $S_z = \pm 1/2$ effective spin, and one immediately understands that the effective Hamiltonian will be a $S = 1/2$ Heisenberg Hamiltonian. If the ground state of the block was a quartet the effective Hamiltonian would be a $S = 3/2$ Heisenberg Hamiltonian. Degenerate ground states of the blocks would imply to handle an orbital degeneracy.

A. From dimers: let a and $\bar{a}$ (resp. b and $\bar{b}$) label the ground state wave functions of the blocks A (resp. B) and E_A and E_B the corresponding eigenenergies. The simplest extraction of the effective interaction between A and B will be obtained from the spectrum of the AB dimer. The model space is composed of the products $\bar{a}b$ and $a\bar{b}$ for $S_z = 0$ and generates a singlet $(a\bar{b} - \bar{a}b)/\sqrt{2}$ and a triplet $(a\bar{b} + \bar{a}b)/\sqrt{2}$. If we know the two eigenstates of AB having the largest projections on the model space, and which are necessarily a singlet Ψ^S_{AB} and a triplet Ψ^T_{AB}, and if we call E^S_{AB} and E^T_{AB} the associated eigenenergies, the effective interactions between the blocks are

- a scalar quantity, equal to $E^T_{AB} - E_A - E_B = R_{AB}$;
- an effective spin coupling of intensity $2J^{eff}_{AB} = E^T_{AB} - E^S_{AB}$.

In general it is hoped that the ground state of AB, and eventually the lowest excited state, are the states of largest projections in the model space. If the former condition is not fulfilled, the definition of the block should be revised. If the second one is not fulfilled the ability of the effective Hamiltonian to reproduce the spin gap of larger systems is questionable.

B. From trimers: one might as well try to extract the interactions from a trimer ABC. The $S_z = 1/2$ model space is spanned by $\bar{a}bc$, $a\bar{b}c$ and $ab\bar{c}$, it generates two doublet states and a quartet state. In full generality the effective Hamiltonian will take the form

$$\begin{array}{c|ccc} \bar{a}bc & -J_{ab} - J_{ac} & J_{ab} & J_{ac} \\ a\bar{b}c & J_{ab} & -J_{ab} - J_{bc} & J_{bc} \\ ab\bar{c} & J_{ac} & J_{bc} & -J_{bc} - J_{ac} \end{array}. \quad (17)$$

It involves 3 spin couplings, the three parameters cannot be determined from the energies of the two doublet states $E^{D_1}_{AB}$ and $E^{D_2}_{AB}$ and of the quartet state E^Q_{AB} of AB having the largest projections in the model space. Let call $\Psi^{D_1}_{AB}$ the lowest doublet. The projection in the model space is

$$P_0\Psi^{D_1}_{AB} = \lambda\bar{a}bc + \mu a\bar{b}c + \nu ab\bar{c}, \quad (18)$$

with $\lambda^2 + \mu^2 + \nu^2 = 1$. It is easy to show that since it is a doublet $\lambda + \mu + \nu = 0$. Hence there is one and only one degree of freedom in the content of this projection. If one wants the effective Hamiltonian to be hermitian, the second doublet state, orthogonal to the lowest one, is entirely determined

$$\Psi^{D_2}_{AB} = \lambda'\bar{a}bc + \mu' a\bar{b}c + \nu' ab\bar{c}, \quad (19)$$

with $\lambda'^2 + \mu'^2 + \nu'2 = 1$; $\lambda' + \mu' + \nu' = 0$; $\lambda\lambda' + \mu\mu' + \nu\nu' = 0$. The effective interactions are obtained from the two energy gaps $E_Q - E_{D_1}$, $E_Q - E_{D_2}$ and from the λ/μ ratio of the first eigenvector, according to the equations.

$$J_{ab} = \lambda(E_Q - E_{D_1})\mu + \lambda'(E_Q - E_{D_1})\mu', \quad (20)$$

$$J_{bc} = \mu(E_Q - E_{D_1})\nu + \mu'(E_Q - E_{D_1})\nu', \quad (21)$$

$$J_{ac} = \lambda(E_Q - E_{D_1})\nu + \lambda'(E_Q - E_{D_1})\nu'. \quad (22)$$

This case illustrates the use of the information contained in the projected eigenvector to define the effective interactions.

Notice that extracting the information from trimers of blocks rather than from dimers

- compels to consider smaller blocks, the practical bottleneck of the method being the exact diagonalization of the oligomer, its size is limited to about 25 sites, C_{25}^{13} spin distributions for $S_z = 1/2$, which means that one may go to 11 sites blocks for dimers, 7 sites blocks for trimers;
- introduces a more sophisticated Hamiltonian, which one may hope to bear more physics;
- requires the identification of more target states, which may sometimes be problematic.

The balance of advantages and inconveniences will be illustrated hereafter.

2.4 Comparison with other recent proposals

One should mention here the recent development of a method, labelled CORE (Contractor Renormalization Group [9]), which makes use of the theory of effective Hamiltonians for the study of periodic lattices. The authors also define blocks and treat oligomers of blocks. They use smaller blocks than we do (usually with even number of sites), but keep more than one block eigenstate to define the model space. The resulting effective Hamiltonians is therefore more complex than the starting one. The method does not maintain the isomorphism exploited in our RSRG version and the algorithm is not iterated, but produces excellent results [10–12].

3 The two-leg ladders with weak ferromagnetic interactions

The present section with apply the RSRG technique to study the spin gap of two-leg ladders and the impact of weak ferromagnetic couplings between adjacent ladders on the spin-gap. The study will proceed first by a study of the F-AF 1-D chain, on which the two-leg ladder well be mapped in a second time.

3.1 The F-AF 1-D chain

The ferro-antiferro (F-AF) simple chain with $J_1 > 0$, $J_2 < 0$ may be characterized by

$$\bar{J} = \frac{J_1 - J_2}{2}, \qquad \delta = \frac{J_1 - J_2}{J_1 + J_2}. \tag{23}$$

The simplest definition of the blocks consists in using $(2n+1)$ sites blocks. They will be coupled either ferromagnetically or antiferromagnetically as evident from Figure 1 where the lowest energy spin distribution has been pictured according to Ovchinnikov [13]. In the dimer-based approach the target vectors are the ground state triplet and the lowest singlet for the ferromagnetically coupled dimer AB, the ground state singlet and the lowest triplet

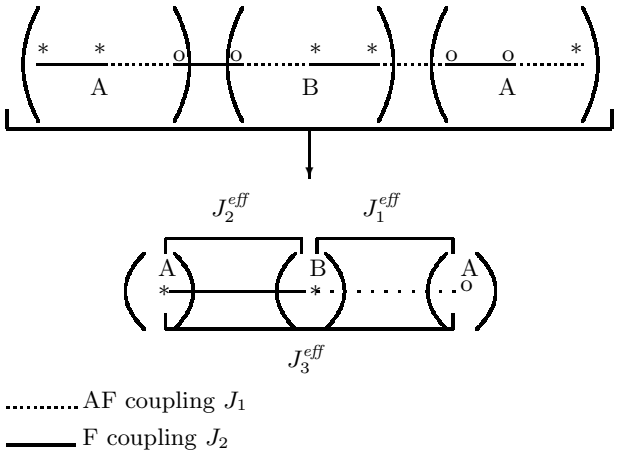

Fig. 1. Principle of the extraction of effective interactions between blocks for a F-AF 1-D chain.

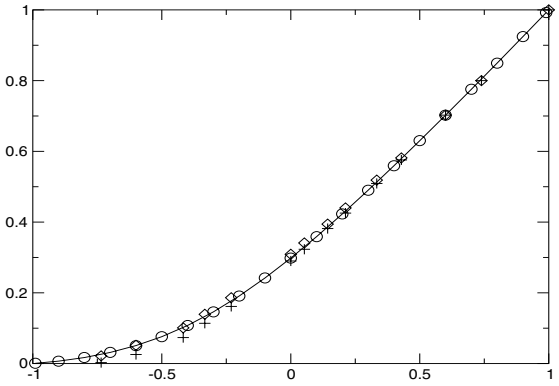

Fig. 2. Dependence the gap for a F-AF 1-D chain on the parameter δ equation (23). Comparison between RSRG-EI ($\circ$), Exact diagonalization [14,15] ($\diamond$), and Pair-DCEFA [16] ($+$).

for the AF coupled dimer BA. They always are the two lowest states. In the trimer-based approach, which also provides a second-neighbor interaction J_3^{eff}, the target space is composed of the two lowest doublet and the lowest quartet states, without ambiguity. Actually the values of J_3^{eff} fall rapidly when the block size increases and the values of the first neighbor interaction are not very different when extracted from the dimer or from the trimer, but the (much smaller) value of the F effective interaction may differ by a factor two.

The extrapolated values of the gap calculated from dimers and trimers are practically indistinguishable (deviation $\sim 0.1\%$) as seen in Figure 2. The results of the method compare excellently with those obtained by extrapolations of exact diagonalization [14,15] and behave more correctly than the Pair-DCEFA [16] approximation in the region $\delta \to -1$.

3.2 Mapping of the two-leg ladder into a ferro-antiferromagnetic chain

The two-leg ladders with AF interactions along the legs $J^{\parallel}$ and the rungs $J^{\perp}$ are known to present a spin gap whatever the $J' = J^{\perp}/J^{\parallel}$ ratio [17–22].

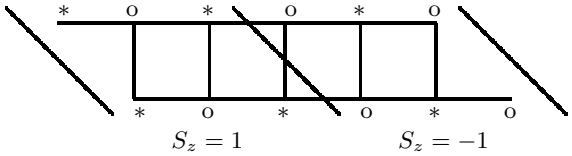

Fig. 3. Mapping the two-leg ladder into a S = 1 AF chain.

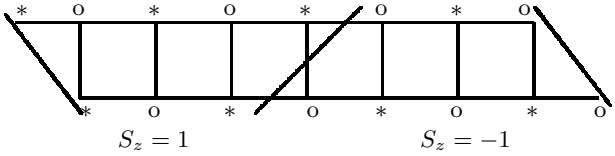

Fig. 4. Alternative mapping of a two-leg ladder into a S = 1 AF chain.

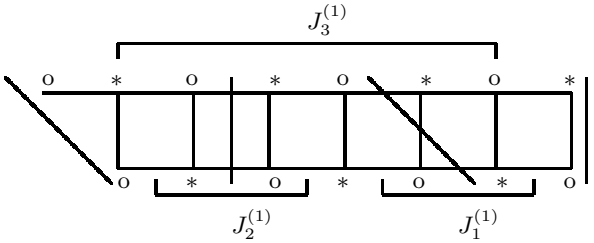

Fig. 5. Mapping of the two-leg ladder in a $S = 1/2$ F-AF chain.

For a two-leg ladder one might define triplet ground state blocks with $(4n + 2)$ sites according to Figure 3. These local triplets will be coupled antiferromagnetically, with equal interactions, and the ladder is mapped into a chain of $S = 1$ blocks, presenting a Haldane gap [23]. A similar mapping is possible with $4n$ sites blocks of a different shape leading to the same conclusion (Fig. 4).

It should be remarked that in such blocks the excited singlet state is low in energy and the bi-quadratic term of the effective Hamiltonian would be quite large.

A more convenient mapping proceeds through the consideration of $(2n + 1)$ sites blocks. The simplest solution consists in a partition into blocks of equal size and shape. As appears clearly from Figure 5 the nearest-neighbor interactions are of alternating ferro and antiferro character.

The ladder is therefore mapped into a F-AF chain, which is gapped, as already discussed. A quantitative application of this mapping has been performed, using either dimers or trimers of blocks. The size of the blocks may be $N_s = 3, 5, 7, 9$ and 11 for dimers, $N_s = 3, 5, 7$ for trimers. One may see in Table 1 that the leading effective interactions is the antiferromagnetic interblock coupling J_1, the values of which is almost the same, for a given size of the blocks, when extracting from dimers or trimers. The value of the ferromagnetic interaction is lower but significantly different when working with trimers. The calculated gap for the mappings from dimers and trimers are reported in Figure 6, after extrapolation on the size-blocks. One may first concentrate on the isotropic case $J^\perp = J^\parallel = 1$, which has been studied by other techniques. From the dimer of blocks after extrapolation on the size of the blocks one obtains a value of $0.530J$. One may mention here that the same value, $0.530J$, is obtained when defining alternating blocks of $(4n + 1)$ and $(4n + 3)$ sites, which leads to a dimerized antiferromagnetic chain (already studied in reference [4] from an RSRG approach). This results illustrates the stability of the method with respect to the design of blocks. A lower result is obtained from the trimers $0.500J$, which is closer to the previously reported values $0.502J$ for Quantum Monte Carlo [24] and $0.504J$ for DMRG [17]. The agreement between all methods is excellent in the region $J^\perp > J^\parallel$ (weakly coupled rungs) as seen in Figure 6. It becomes more problematic in the region of weakly coupled AF legs $J^\perp < J^\parallel$. The gap calculated from the dimers increases instead of stabilizing close to $0.41J^\perp$. It is easy to understand that the mapping becomes irrelevant in this domain since the ground state of the $(2n+1)$ sites blocks becomes the product of a singlet on a leg and of a doublet on the other one (cf. Fig. 7). The interactions prevail along the legs and the second-neighbor interaction

Table 1. Effective interactions between blocks of various sizes (N_s) for the mapping of a two-leg ladder ($J^\parallel = J^\perp = 1$) on a F-AF chain, extracted from either dimers or trimers.

N_s	dimers	trimers
3	$J_1^{(1)} = 0.819190$	$J_1^{(1)} = 0.824305$
	$J_2^{(1)} = -0.333230$	$J_2^{(1)} = -0.344646$
		$J_3^{(1)} = 0.276585$
5	$J_1^{(1)} = 0.713618$	$J_1^{(1)} = 0.696924$
	$J_2^{(1)} = -0.201050$	$J_2^{(1)} = -0.106358$
		$J_3^{(1)} = 0.111677$
7	$J_1^{(1)} = 0.651990$	$J_1^{(1)} = 0.630380$
	$J_2^{(1)} = -0.105133$	$J_2^{(1)} = -0.060201$
		$J_3^{(1)} = 0.052666$
9	$J_1^{(1)} = 0.614038$	
	$J_2^{(1)} = -0.054940$	
11	$J_1^{(1)} = 0.589050$	
	$J_2^{(1)} = -0.028920$	

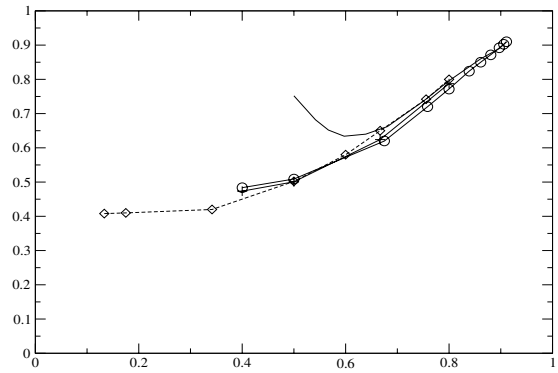

Fig. 6. Calculated spin gap for a two-leg ladder as a function of the $\frac{J^\perp}{J^\parallel + J^\perp}$ ratio, in $J^\perp$ units. ($\diamond$) Quantum Monte Carlo [24], (-) Perturbative estimate [25], ($\circ$) this work with AF-F mapping from of identical $(2n + 1)$ sites blocks, (+) this work, same mapping, effective interactions form trimers.

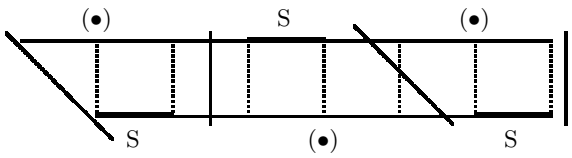

Fig. 7. Prevalence of the 2nd neighbor interactions for weakly coupled legs.

between the doublets A and C, localized on the same leg, becomes dominant. The mapping from the trimers takes this interaction into account and the calculated gap has a qualitatively correct behavior, keeping a constant value for $J^{\perp} < J^{\parallel}$. The calculated value, $0.5J^{\perp}$, is larger than the correct one ($0.41J^{\perp}$) but the behavior of the gap is correct. This is a case where considering trimers instead of dimers improves the quantitative and qualitative performances of the method, but the physical origin of the superiority of the trimers in this case is clear.

3.3 Ferromagnetically coupled two-leg ladders

Several studies have been performed concerning weakly coupled two-leg ladders, either ferromagnetically or antiferromagnetically [15,26]. However in these studies, each site of a ladder is only coupled with one site of the neighbor ladder. The physics of the interactions is different for the $SrCu_2O_3$ lattice which can be seen as independent planes containing parallel two-leg ladders but where the adjacent ladders are translated by half of the on-leg Cu-Cu distance, and the distance between the legs of adjacent ladders is small [27]. Recent ab initio calculations [28] have predicted a ferromagnetic interaction J^{int} to exist between the closest Cu atoms of distinct ladders. These calculations also predict a ratio $J^{\perp}/J^{\parallel} = 0.9$, i.e., close to 1. One may mention the controversy regarding the $J^{\perp}/J^{\parallel}$ ratio, which originates in the fact that using a simple Heisenberg Hamiltonian for an isolated ladder the interpretation of some experiments suggests $J^{\perp}/J^{\parallel} = 1$, while other properties require a much smaller ratio $J^{\perp}/J^{\parallel} = 0.5$. A possible explanation of this discrepancy had to be searched in the neglect of either four-body operators, which may be important in plaquettes [29–33], or of interladders interactions.

Recent works have shown that

- the influence of 4-body operators on the gap may be rather large [34],
- the amplitude of the 4-body operator is much larger in ladders than in La_2CuO_4 2-D lattice, according to accurate ab initio calculations performed along the same methodology [35,36],
- the interladder interactions have a weak impact on the gap [37], at least for the proposed ratios of the J's.

We have nevertheless calculated this last influence using our method, in order to compare with this last result [37]. We have defined similar $(2n+1)$ sites blocks on ladders, which transform them into F-AF chains, and have determined effective interactions between blocks belonging to different ladders. This extraction rests on the consideration of tetramers of $N_s = 5$ sites. Two types of tetramers have to be considered (Fig. 8). Taking $J^{\parallel} = J^{\perp} = 1$, $J^{int} = -J^{\parallel}/5$ (as suggested by Ref. [23]) one obtains ${J_1}^{(1)} = 0.7122$, ${J_2}^{(1)} = -0.2002$, ${J_3}^{(1)} = -0.01614$, ${J_4}^{(1)} = -0.0346$, ${J_5}^{(1)} = 0.01462$, all other interactions including the four-blocks operators being smaller than 10^{-2}. The values of J_1 and J_2 compare well with those obtained from dimers in the isolated ladder $J_1^{(1)} = 0.7136$, $J_2^{(1)} = -0.2010$, for same size blocks. Then one may study various rectangular clusters of blocks, belonging to either one, two, three or four ladders, with a total number of 20 blocks. A double extrapolation on the length and width of these rectangles leads to the conclusion that the lowering of the gap by the interladder interactions is $-0.035J^{\parallel} = +0.21J^{int}$. This result is in agreement with the recent result of reference [33], and confirms that the contradictions faced by the interpretation in terms of a simple $J^{\parallel}/J^{\perp}$ Heisenberg Hamiltonian cannot be solved by introducing the interladder interactions.

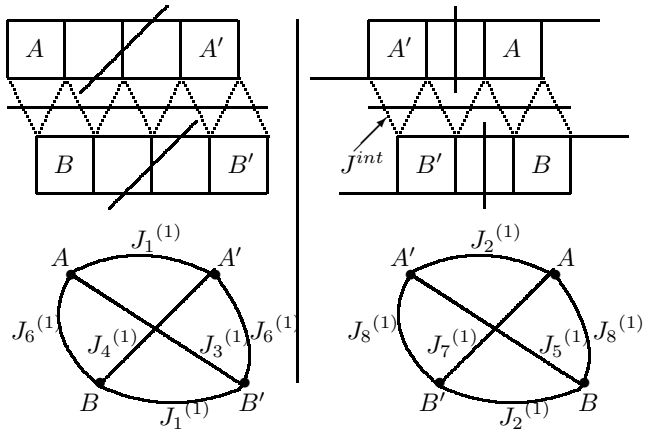

Fig. 8. Definition of the effective interactions in the RSRG treatment of coupled two-leg ladders.

4 The 1/5-depleted Heisenberg square lattice revisited

The 1/5-depleted spin square lattice has received some attention from theoreticians during the last decade since it was supposed to represent correctly the CaV_4O_9 lattice, which presents a spin gap. It happened that the 1-3 interactions between next-nearest neighbor atoms are important, but the simple lattice pictured in Figure 9, composed of plaquettes and bonds, already presents an interesting physics. Accurate Quantum Monte Carlo calculations [38] confirm the suggestion of perturbative approaches [39], namely the existence of three phases, when the ratio of the spin coupling in the plaquette J_p to the coupling in the bonds J_d varies. One may take $\lambda = J_p/(J_p + J_d)$ as a parameter, varying between 0 and 1. For strong values of λ the lattice can be seen as composed of weakly interacting plaquettes.

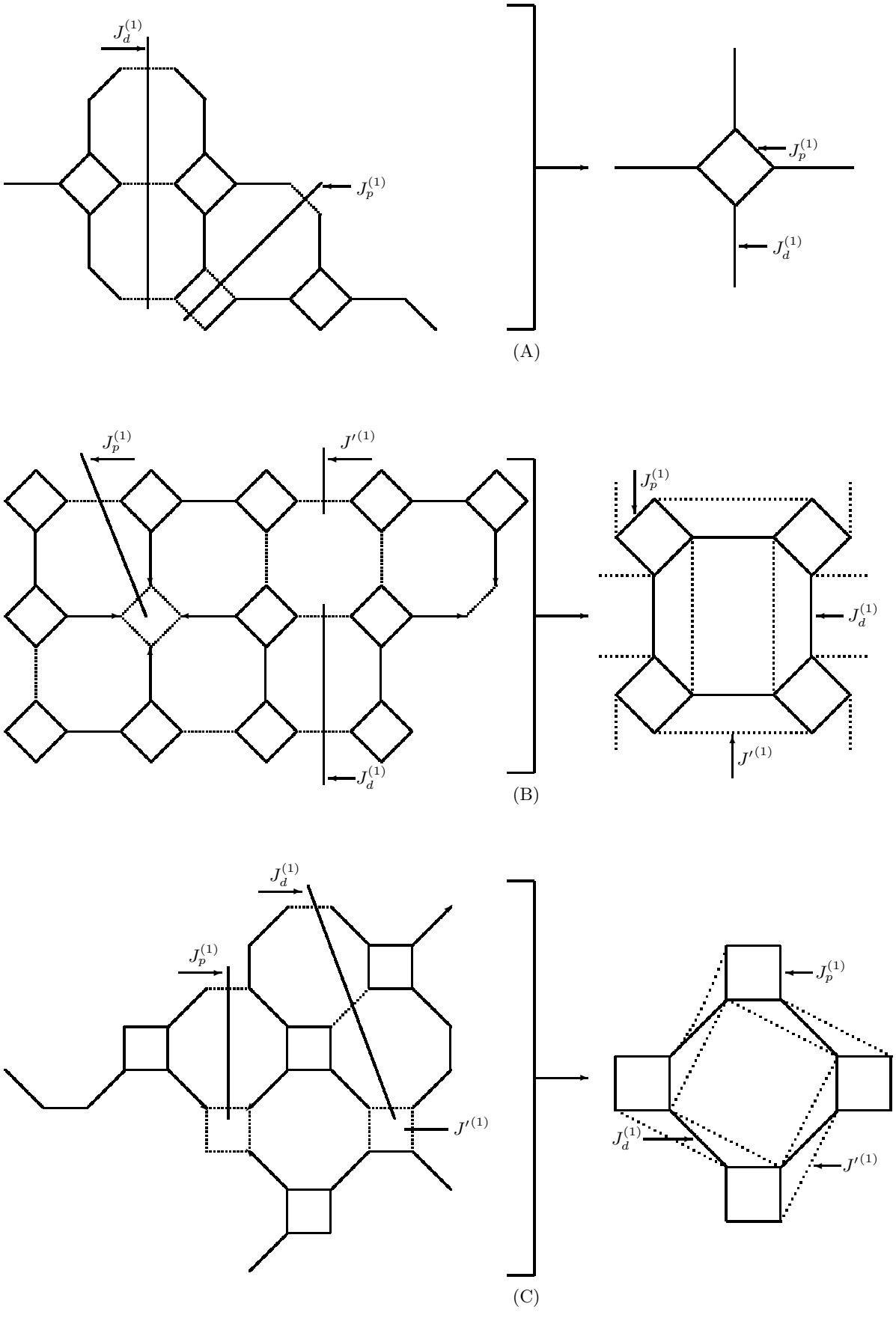

Fig. 9. Definition of 9 sites blocks leading to isomorphic lattices in the 1/5-depleted square lattice.

When λ is small the dimer singlets on bonds are weakly coupled. In between the lattice can be seen as a Néel ordered phase surviving to the depletion. QMC calculations locate the critical ratios between the dimer phase and the Néel ordered phase at $0.55 < J_p/J_d < 0.65$ and between the Néel ordered phase and the plaquette phase at $1.05 < J_p/J_d < 1.10$. The plaquette and the dimer phase present a spin gap, while the Néel ordered phase is gapless. These results agree with the earlier perturbative treatments [39]. We have tempted to study this system using the RSRG-EI technique.

We first have identified 9 sites blocks which maintain the original lattice along the iterations. Three of them are pictured in Figure 9. The first one preserves the stoichiometric ratio (equal to 2) of the number of plaquette versus bond interactions, and the simplicity of the interactions is maintained at each step.

In the second definition the blocks involve 2 plaquettes ($8J_p$ interactions) and two bonds ($2J_d$ interactions). This definition should be especially convenient for the $J_p > J_d$ regime where it lets a unique unpaired electron, and should become irrelevant for weak J_p/J_d ratios. The third definition is expected to be relevant in the weak J_p/J_d regime since the blocks involve $4J_d$ and $5J_p$ and let only one unpaired electron when J_p tends to zero. It should fail in the strong J_p/J_d regime. Figure 10 pictures the energies of the different blocks as a function of $J_p/(J_p + J_d)$ and it appears that

- the stoichiometric blocks are never those of lower energy;
- the second type of blocks is the one of lowest energy for $J_p/(J_p + J_d) > 0.427$.

Figure 9 also represents the interactions between the blocks. In the three partitions the identification of plaquettes of blocks and of dimer interactions between them appears clearly. However while the stoichiometric blocks do not introduce 2nd neighbor interactions between blocks this is no longer true for the two other partitions. These interactions remain much weaker than the nearest-neighbor ones. Notice that in the 2nd and 3rd definitions tetramers of blocks define a kind of vortex, and that in the 2nd definition one has used vortices of opposite rotation direction. One shall call $J_p^{(1)}$ the effective coupling between blocks belonging to the same plaquette of blocks and $J_d^{(1)}$ the interaction between blocks belonging to adjacent plaquettes of blocks. Figure 11 represents the ratio $\lambda^{(1)} = J_p^{(1)}/(J_p^{(1)} + J_d^{(1)})$ as a function of λ. The results deserve the following comments

- starting from the stoichiometric blocks, one obtains two zones, one for $\lambda < 0.438$ in which iterating the process will tend to the $\lambda = 0$ ($J_p = 0$) accumulation point, i.e., to non interacting dimers. For $\lambda > 0.438$ the accumulation point corresponds to $\lambda = 1$, i.e., to non interacting plaquettes. For $\lambda_c = 0.438$ one has a fixed repulsive point, for which the ratio $\lambda^{(n)}$ is constant at all iterations. Since $J_p^{(1)}$ and $J_d^{(1)}$ are lower than 1, the gap decreases at each iteration, so that there is no spin gap at this precise point. As clear from Figure 11, since the attractive fixed points are reached in a finite number of iterations when $\lambda \neq \lambda_c$, the model predicts non zero gaps for both the dimer phase $0 < \lambda < \lambda_c$ and the plaquette phase $\lambda_c < \lambda < 1$. The gapless phase is reduced to a single value of λ;
- starting from the second and third definitions of the blocks one observes a non-monotonic behavior of $\lambda^{(1)} = f(\lambda)$. The distance of $\lambda^{(1)}$ to the straight line of slope 1 (i.e., the quantity $|\lambda^{(1)} - \lambda|$) goes through a minimum for both definitions of the blocks. We have previously observed such a behavior in the study of the 1-D frustrated chain, when varying the ratio $\lambda = j/J$ of the 2nd neighbor interaction j to the 1st neighbor interaction J. Calculating the effective interaction $J^{(1)}$ and $j^{(1)}$ between blocks and the ratio $\lambda^{(1)}(\lambda)$, the quantity $\lambda^{(1)}(\lambda) - \lambda$ goes through a minimum for $\lambda \simeq 0.24$, near the well-known 2nd-order phase transition. Increasing the size of the blocks we observed that the minimal value of $\lambda^{(1)}(\lambda) - \lambda$ tends to zero. It is not possible in the 2-D lattices to perform such an extrapolation on the block size, but one may consider that the existence of a minimum in the quantity $\lambda^{(1)} - \lambda$ is a signature of a phase transition and the

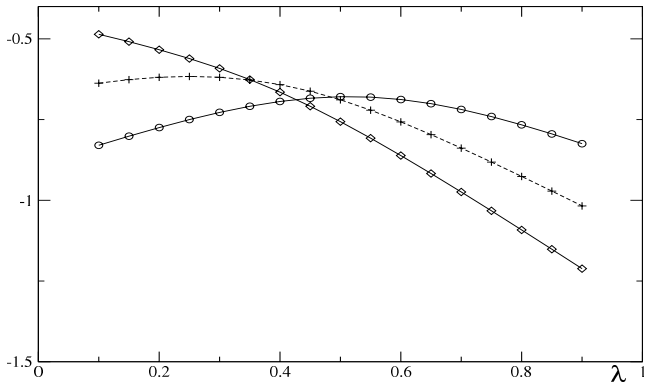

Fig. 10. Block energies (per atom) for the 3 definitions of the blocks given in Figure 9, as functions $\lambda = J_p/(J_p + J_d)$. Definition A (+), definition B ($\diamond$), and definition C ($\circ$).

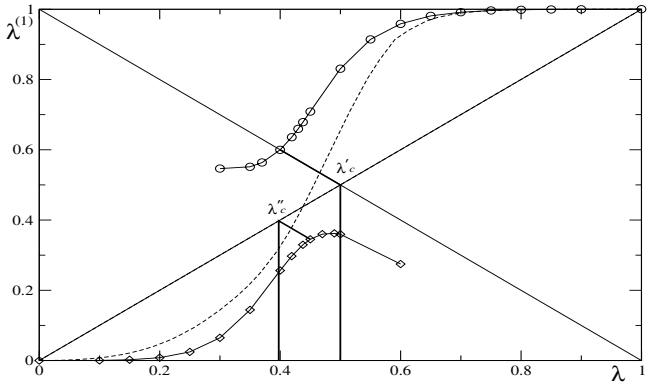

Fig. 11. Evolution of the ratio $\lambda^{(1)} = J_p^{(1)}/(J_p^{(1)} + J_d^{(1)})$ as a function of $\lambda = J_p/(J_p + J_d)$, for three definitions of the blocks (cf. Fig. 9). (-) definition A, ($\circ$) definition B, and ($\diamond$) definition C. The values λ_c' and λ_c'' identify the critical ratios.

extrapolated critical value of the parameter may be estimated as $\lambda'_c = (\lambda^{(1)} + \lambda)/2$ for the value of λ which minimizes $|\lambda^{(1)} - \lambda|$ (i.e., $\partial(\lambda^{(1)} - \lambda)/\partial\lambda = 0$). One obtains so $\lambda'_c = 0.500$ ($J_p^{(1)}/J_d^{(1)} = 1.000$) and $\lambda''_c = 0.398$ ($J_p^{(1)}/J_d^{(1)} = 0.660$) which should be the lower and upper limits of the gapless phase. These values compare quite well with those proposed from the previously mentioned perturbative [39] or Quantum Monte Carlo [38] treatments.

5 Phase transition in the 2-D spin frustrated Shastry-Sutherland lattice

The $SrCu_2(BO_3)_2$ crystal can be seen as built of rather distant planes of $CuBO_3$ units. The Copper ions have a d^9 electronic structure and bear a $S = 1/2$ spin. Figure 12 schematizes the in-plane structure of this material ($J_3 = 0$). The Copper atoms are strongly coupled (through J_2) into dimer singlets. The interactions J_1 with the four other neighbors is smaller than J_2. This system has attracted much attention (for a review see Ref. [40]), and is known as the Shastry-Sutherland lattice, the properties of which depend an the J_1/J_2 ratio. When $J_1/J_2 = \alpha$ is smaller than a critical value α_c, the ground state is a pure product of bond singlets. For α tending to infinity the lattice becomes a simple 2-D lattice, the ground state is a Néel-ordered phase. At least one phase transition occurs for a value of $\alpha \sim 0.67 - 0.70$ (see below).

The RSRG-EI method has been employed to study the phase transition in this system, starting from 9 sites "square" blocks pictured in Figure 12. They define an isomorphic lattice at each step. If one calls $\mu = J_1/(J_1 + J_2)$, the first iteration defines a ratio $\mu^{(1)} = J_1^{(1)}/(J_1^{(1)} + J_2^{(1)}) = f(\mu)$. Figure 13 gives the evolution of $\mu^{(1)}$ in the $\alpha > 0.666$ ($\mu > 0.4$) regime.

One sees that, for $\alpha_c = 0.69583$ ($\mu_c = 0.41032$), $\alpha^{(1)} = \alpha$ ($\mu^{(1)} = \mu$). This represents a fixed point of the problem. For $\mu > \mu_c$ the ratio $\mu^{(n)}$ increases at each iteration, going to the $\mu = 1$ accumulation point in an infinite number of steps since $(\partial\mu^{(1)}/\partial\mu) \neq 0$ (actually close to 0.5) when $\mu \to 1$. Hence the system is gapless for $\alpha > \alpha_c$. For $\alpha < \alpha_c$, $\alpha^{(1)}$ becomes larger than α_c, the procedure diverges since it becomes impossible to identify the target eigenvectors. This value of the critical ratio α_c should be compared with other estimates. Exact diagonalizations [41] up to 20 sites led to 0.70, Ising expansion [42] to 0.691 and a dimer expansion [43] to 0.697. Further works have suggested that this phase transition concerns a intermediate phase which would be based on either plaquette singlets ($\alpha_c = 0.677$) according to a plaquette expansion [44] or 0.67 from exact diagonalizations [45] up to 32 sites, or columnar [46] ($\alpha_c = 0.69$). Our calculation does not allow us to identify an intermediate phase, the existence of which remains under discussion [40].

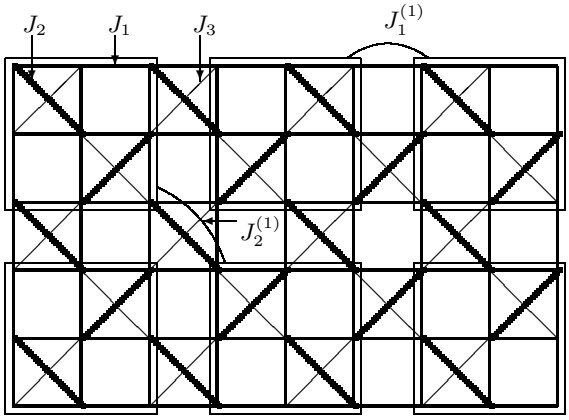

Fig. 12. Schematic representation of partially frustrated 2-D square lattices. The Shastry-Sutherland lattice corresponds to $J_3 = 0$. In the checkerboard lattice $J_3 = J_2$. Definition of the blocks and of their effective interactions.

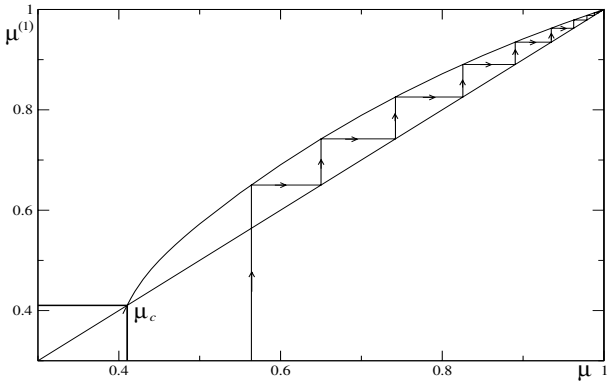

Fig. 13. Evolution of the first iteration ratio $\mu^{(1)} = J_1^{(1)}/(J_1^{(1)} + J_2^{(1)})$ as a functions of $\mu = J_1/(J_1 + J_2)$ for the Shastry-Sutherland lattice. The phase transition appears for $\mu^{(1)} = \mu$ at μ_c. The stairs illustrate the steps of the iteration RSRG toward the ($J_2 = 0$) non-frustrated 2-D accumulation point, and the gapless character of this phase.

We have calculated the cohesive energy for $\alpha > \alpha_c$. Writing the Hamiltonian as

$$H = \sum_{\langle i,j\rangle_{NN}} 2J_2(S_iS_j - 1/4) + \sum_{\langle k,l\rangle_{NN'}} 2(1-J_2)(S_kS_l - 1/4), \tag{24}$$

where NN and NN' represent the couples of atoms connected by $J_2 = 1 - J_1$ and J_1 respectively, the cohesive energy in the gapless phase is almost a linear function of μ, which goes to -2.33231 for $\mu = 1$ (the most accurate QMC [47] value being -2.33868). With this definition of the Hamiltonian the energy of the product of bond singlets is equal to -1 whatever J_1/J_2. The energy obtained from RSRG-EI iterations is plotted in Figure 14. The consistence of the two independent criteria

- $\mu^{(1)} = f(\mu)$ (Fig. 13);
- crossing of the cohesive energies $E_{coh} = f(\mu)$ (Fig. 14) is very good.

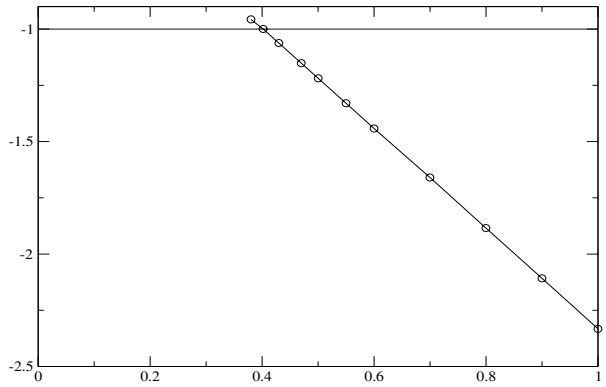

Fig. 14. Cohesive energy of the Shastry-Sutherland lattice as a function of μ (cf. Fig. 13).

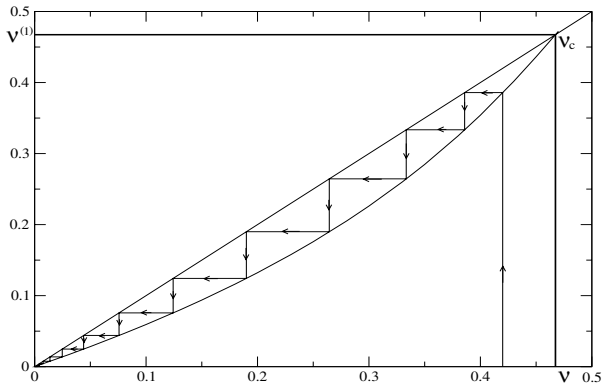

Fig. 15. Evolution of the first iteration ratio $\nu^{(1)} = J_2^{(1)}/(J_1^{(1)} + J_2^{(1)})$ as a function of $\nu = J_2/(J_1 + J_2)$ for the checkerboard lattice.

The first one gives $\alpha_c = 0.69583$, which for the second $\alpha_c = 0.67224$. This example shows the consistence and relevance of the method in the study of a 1st-order phase transition in a frustrated 2-D lattice.

6 The Néel/dimer phase transition in the J_2/J_1 checkerboard lattice

The checkerboard lattice (as defined from Fig. 12 when $J_2 = J_3$) can be studied as a function of the (J_2/J_1) ratio between the diagonal spin coupling J_2 appearing in one square over two and the spin coupling J_1 occurring on the bonds of the square 2-D lattice. Pyrochlore lattices are a real material (3-D) where the ratio J_2/J_1 is equal to 1. In this regime the checkerboard (or 2-D pyrochlore) lattice is known to be in a dimer-phase [48,49]. For $J_2 = 0$ the lattice is a simple 2-D square lattice, in a simple Néel-ordered gapless phase and a phase transition should occur in the interval $0 < J_2/J_1 < 1$. We have again used square (3×3) blocks of 9 sites. The new lattice is isomorphic to the starting one (cf. Fig. 12) producing $J_1^{(1)}$ and $J_2^{(1)}$. The evolution of the ratio $\nu^{(1)} = J_2^{(1)}/(J_1^{(1)} + J_2^{(1)})$ as a function of a $\nu = J_2/(J_1 + J_2)$ is plotted in Figure 15. One sees that a critical value of ν appears for $J_2 = 0.8774 J_1$ ($\nu = 0.46735$) for which $J_2^{(1)}/J_1^{(1)} = J_2/J_1$. Below this critical ratio the system is gapless, since the accumulation point $\nu = 0$ (simple 2-D square lattice) is reached from the starting ν value in an infinite number of steps, the slope $(\partial\nu^{(1)}/\partial\nu)_{\nu=0}$ being different from zero at the origin.

7 Conclusion

The present work shows the efficiency of the combined use of the effective Hamiltonian theory and of the Real Space Renormalization Group for the study of periodic spin lattices. The main idea consists in defining periodisable blocks in the lattice, with odd number of sites, (or with even number of sites, but such that the ground state of the blocks is not a singlet state). The block can than be viewed as a pseudo-spin. The effective interactions between these pseudo-spins can be determined accurately by solving the Schrodinger equations for dimers or trimers of blocks, and by using the Bloch's effective Hamiltonian theory, which uniquely defines the effective interactions from the knowledge of the most relevant eigenenergies and eigenvectors of the starting Hamiltonian. This basic idea, which introduces effective interactions between the ground state of the blocks, is general, and can be employed with other types of starting Hamiltonians, which may be of Hubbard type, or even the exact Hamiltonians. These inter-block effective interactions can be used along different strategies, one may define blocks of blocks and dimers or trimers of blocks of blocks, and repeat the research of the effective interactions between blocks of blocks till the convergence of the procedure. Following the philosophy of the Wilson's Real Space Renormalization Group (RSRG), one generates a RSRG variant (RSRG-EI) which renormalizes the interactions [4], while the original version consisted in a simple truncation of the Hilbert space. The present work has confirmed the efficiency of the RSRG-EI method illustrated in reference [4]. It has explored the stability of the results with respect to some degrees of freedom of the method, namely

- the mode of extraction of the effective interactions, from dimers or trimers of blocks. Dividing a superblock into three blocks rather than into two blocks, for the same size of the superblock, implies a reduction of the size of the blocks, the consideration of more eigenstates of the superblocks, hence the consideration of more physics, but also a complexification of the effective interactions. The use of trimers may give better results than that of dimers, as seen in the case of two-leg ladders for small rung interactions. Logical arguments enable to decide whether the definition of the original interactions requires the consideration of trimers rather than of dimers;
- the design of the elementary blocks. Two types of partitions into blocks have been considered for the two-leg ladders, one mapping into a F-AF 1-D chain, the other

one into a dimerized AF 1-D chain, which lead to consistent results.

A possible interest of the RSRG-EI method, compared to the DMRG, which is certainly of better accuracy but essentially limited to 1-D systems, is its applicability to 2-D and even 3-D lattices. As a first example the present paper has studied the impact on the gap of a ferromagnetic coupling between Cu atoms of adjacent ladders in the Sr_2CuO_3 2-D lattice. The RSRG-EI calculation confirms the very limited effect of this interaction between ladders.

A second application concerns the 1/5-depleted square spin lattice, where the design of different 9 sites blocks which keep the structure of the original lattice helps to identify phase transitions. Of course the 2-D spin non-frustrated lattices can be efficiently studied by Quantum Monte Carlo techniques, which are very accurate. But QMC calculations are not possible on spin-frustrated lattices. The here-proposed study of the phase transition in the Shastry-Sutherland lattice and on the checkerboard lattice shows that the RSRG-EI technique, which does not suffer such a limitation, may furnish useful and reliable informations on such systems as well.

The authors thank D. Poilblanc and S. Capponi for helpful discussions.

References

1. K.G Wilson, Rev. Mod. Phys. **47**, 773 (1975)
2. S.R. White, Phys. Rev. B **48**, 10345 (1993)
3. S.R. White, Phys. Rev. Lett. **69**, 2863 (1992)
4. N. Guihéry, J.P. Malrieu, Phys. Rev. B **63**, 085110 (2001)
5. C. Bloch, Nucl. Phys. **6**, 329 (1958)
6. P. Durand, J.P. Malrieu, in *Ab initio Methods in Quantum Chemistry I,* edited by K.P. Lawley (Wiley, New York, 1987), p. 320
7. J. des Cloizeaux, Nucl. Phys. **20**, 321 (1960)
8. M.B. Lepetit, E. Manousakis, Phys. Rev. B **48**, 1028 (1993)
9. C.J. Morningstar, M. Weinstein, Phys. Rev. D **54**, 4131 (1996)
10. M. Weinstein, Phys. Rev. B **63**, 174421 (2001)
11. E. Altman, A. Auerbach, Phys. Rev. B **65**, 104508 (2002)
12. S. Capponi, D. Poilblanc, Phys. Rev. B **66**, 180505(R) (2002)
13. Ovchinnikov, Theor. Chim. Acta **47**, 297 (1978)
14. K. Hida, Phys. Rev. B **45**, 2207 (1992)
15. S. Dalosto, J. Riera, Phys. Rev. B **62**, 928 (2000)
16. S. Kokado, N. Suzuki, J. Phys. Soc. Jpn **66**, 3605 (1997)
17. S.R. White, R.M. Noack, D.J. Scalapino, Phys. Rev. Lett. **73**, 886 (1994)
18. E. Dagotto, J. Riera, D.J. Scalapino, Phys. Rev. B **45**, 5744 (1992)
19. S.P. Strong, A.J. Millis, Phys. Rev. Lett. **69**, 2419 (1992)
20. T. Barnes, E. Dagotto, J. Riera, E.S. Swanson Phys. Rev. B **47**, 3196 (1993)
21. T.M. Rice, S. Gopalan, M. Sigrist, Europhys. Lett. **23**, 445 (1993)
22. G. Sierra, J. Phys. A **29**, 3299 (1996)
23. F.D.M. Haldane, Phys. Lett. A **93**, 464 (1983)
24. M. Greven, R.J. Birgeneau, U.-J. Wiese, Phys. Rev. Lett. **77**, 1868 (1996)
25. M. Reigrotzki, H. Tsunetsugu, T.M. Rice, J. Phys. C **6**, 9235 (1994)
26. J. Tworzydlo, O.Y. Osman, C.N.A. Van Duin, J. Zaanen, Phys. Rev. B **59**, 115 (1999)
27. Z. Hiroi, M. Azuma, M. Takano, Y. Bando, J. Solid State Chem. **95**, 230 (1991)
28. C. de Graaf, I. de P.R. Moreira, F. Illas, R.L. Martin, Phys. Rev. B **60**, 3457 (1999)
29. C.J. Calzado, J.P. Malrieu, Phys. Rev. B **69**, 094435 (2004)
30. J.P. Malrieu, D. Maynau, J. Am. Chem. Soc. **104**, 3021 (1982)
31. A.H. MacDonald, S.M. Girvin, D. Yoshioka, Phys. Rev. B **37**, 9753 (1988)
32. M. Roger, J.M. Delrieu, Phys. Rev. B **39**, 2299 (1989)
33. J. Lorenzana, J. Eroles, S. Sorella, Phys. Rev. Lett. **83**, 5122 (1999)
34. S. Brehmer et al., Phys. Rev. B **60**, 329 (1999)
35. C.J. Calzado, J.P. Malrieu, Eur. Phys. J. B **21**, 375 (2001); C.J. Calzado, J.P. Malrieu, Phys. Rev B **63**, 214520 (2001)
36. C.J. Calzado, C. de Graaf, E. Bordas, R. Caballol, J.P. Malrieu, Phys. Rev. B **67**, 132409 (2003)
37. D.C. Johnston et al. `cond-mat/0001147` (unpublished)
38. M. Troyer, H. Kontani, K. Ueda, Phys. Rev. Lett. **76**, 3822 (1996)
39. K. Ueda, H. Kontani, M. Sigrist, P.A. Lee, Phys. Rev. Lett. **76**, 1932 (1996)
40. S. Miyahara, K. Ueda, J. Phys.: Condens. Matter. **15**, R327 (2003)
41. S. Miyahara, K. Ueda, Phys. Rev. Lett. **82**, 3701 (1999)
42. Z. Weihong, J. Oitmaa, C.J. Hamer, Phys. Rev. B **60**, 6608 (1999)
43. E. Müller-Hartmann, R.R.P. Singh, C. Knetter, G.S. Uhrig, Phys. Rev. Lett. **84**, 1808 (2000)
44. A. Koga, N. Kawakami, Phys. Rev. Lett. **84**, 4461 (2000)
45. A. Läuchli, S. Wessel, M. Sigrist, Phys. Rev. B **66**, 014401 (2002)
46. Z. Weihong, J. Oitmaa, C.J. Hamer, Phys. Rev. B **65**, 014408 (2002)
47. K.J. Runge, Phys. Rev. B **45**, 12292 (1992)
48. S.E. Palmer, J.T. Chalker, Phys. Rev. B **62**, 488 (2000)
49. S.E. Palmer, J.T. Chalker, Phys. Rev. B **64**, 094412 (2001)